PHYSICAL REVIEW B **80**, 100401(R) (2009)

Anomalous Hall effect in the t_{2g} orbital kagome lattice due to noncollinearity: Significance of the orbital Aharonov-Bohm effect

Takeshi Tomizawa and Hiroshi Kontani
Department of Physics, Nagoya University, Furo-cho, Nagoya 464-8602, Japan
(Received 4 February 2009; revised manuscript received 26 July 2009; published 9 September 2009)

A mechanism of spin structure-driven anomalous Hall effect (AHE) in tilted ferromagnetic metals is proposed by taking account of the *d*-orbital degree of freedom. We find that a conduction electron acquires a Berry phase due to the complex *d*-orbital wave function, in the presence of noncollinear spin structure and the spin-orbit interaction. The AHE driven by this orbital-derived Berry phase is much larger than the AHE induced by spin chirality, and it naturally explains the salient features of spin structure-driven AHE in pyrochlore $Nd_2Mo_2O_7$. Since the proposed AHE can occur even for coplanar spin orders (M_z=0), it is expected to emerge in other interesting geometrically frustrated systems.

DOI: 10.1103/PhysRevB.80.100401 PACS number(s): 72.10.−d, 72.80.Ga, 72.25.Ba

Recently, intrinsic anomalous Hall effect (AHE) attracts renewed attention as an interesting quantum transport phenomenon in multiband metals. It is independent of the quasiparticle damping rate γ as shown by Karplus and Luttinger (KL).[1] Recently, the theory of KL had been developed intensively, and quantitative studies had been performed for *f*-electron systems,[2] *d*-electron systems,[3,4] and two-dimensional Rashba electron-gas model.[5,6] The origin of giant AHE realized in *d*(*f*)-electron systems is the "orbital Aharonov-Bohm (AB) effect," in which the complex phase factor arises from the *d*(*f*) angular momentum that is revived by the strong atomic spin-orbit interaction (SOI).[2,4,7–10] In *d*(*f*)-electron systems, strong entanglement of orbital and spin degrees of freedom in multiband Bloch function gives rise to the prominent Berry curvature.[11,12]

Especially, the AHE due to nontrivial spin structure attracts increasing attention, in accordance with the recent development of the study of frustrated systems. The AHE induced by the Berry phase associated with spin chirality had been discussed for Mn oxides,[13] pyrochlore compounds (kagome lattice),[14,15] and in spin glass systems.[16] Metallic pyrochlore $Nd_2Mo_2O_7$ would be the most famous experimental candidate:[17–20] below T_c=93 K, Mo 4*d* electrons are in the ferromagnetic state. Below $T_N \approx 30$ K, localized Nd 4*f* electrons form noncoplanar spin-ice magnetic order, and the tilting of Mo moment θ is induced by *d*-*f* exchange interaction, as shown in Fig. 1. The chirality-driven anomalous Hall conductivity (AHC) is proportional to $\boldsymbol{s}_A \cdot (\boldsymbol{s}_B \times \boldsymbol{s}_C) \propto \theta^2$ in the weak exchange coupling near half filling.[14,15] However, the neutron-diffraction experiments[18] had shown that $\theta^2 \ll 10^{-3}$, suggesting that the chirality-driven AHC is very small. Moreover, the field dependences of the AHC and θ^2 are quite different.[18]

In previous studies,[13–15] *s*-orbital models had been studied. However, it is natural to expect a significant role of the orbital degree of freedom on the spin structure-driven AHE, as in the case of the conventional KL-type AHE in *d*-electron systems.[2,4,7–9]

In this Rapid Communication, we find that the Berry phase is induced by the complex *d*-orbital wave function in tilted ferromagnetic metals, and it causes a prominent spin structure-driven AHE. In $Nd_2Mo_2O_7$, the AHE due to orbital Berry phase is much larger than the chirality-driven AHE since the former is *linear in* θ consistently with experiments. In contrast, both the conventional KL term in simple ferromagnets ($\propto M_z \propto \cos\theta$) and the spin chirality term cannot have θ-linear terms. The present orbital mechanism will be realized not only in other pyrochlore $Pr_2Ir_2O_7$,[20] but also in various geometrically frustrated metals.

Here, we construct the t_{2g} tight-binding model for Mo 4*d* electrons. For this purpose, we consider the spinel structure (XMo_2O_4) instead of pyrochlore structure ($X_2Mo_2O_7$). In both structures, Mo atoms form the same pyrochlore lattice. The location of O atoms in spinel is rather easy to treat

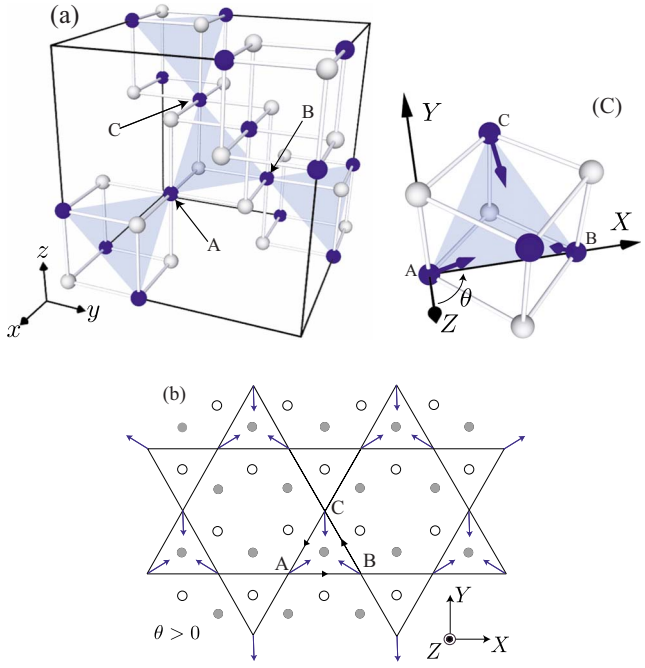

FIG. 1. (Color online) (a) Spinel crystal structure. Blue (white) circles are Mo (O) ions. The Mo ions on the [111] plane form the kagome lattice. (b) Kagome lattice made of Mo ions. White (gray) circles are O ions above (below) the Mo layer. A unit cell contains sites *A*–*C*. (c) Umbrellalike local exchange field at Mo sites represented by arrows.

theoretically, and the difference is not essential for later study, as we discuss later. Figure 1(a) represents the Mo atoms (black circles) and O atoms (white circles) in the spinel structure. The [111] Mo layer and the surrounding O atoms in the spinel structure are extracted in Fig. 1(b), where the white (gray) circles represent the O atoms above (below) the Mo layer. We study this kagome lattice t_{2g}-orbital tight-binding model, where the principal axis for the Mo d orbital is fixed by the surrounding O_6 octahedron. A vector (n_x,n_y,n_z) in the xyz coordinates in Fig. 1(a) is transformed into $[n_X,n_Y,n_Z]$ in the XYZ coordinates in Fig. 1(b) as $(n_x,n_y,n_z)=[n_X,n_Y,n_Z]\hat{O}$, where the coordinate transform matrix $\hat{O}$ is given by

$$\hat{O}=\frac{1}{\sqrt{6}}\begin{pmatrix}-\sqrt{3} & \sqrt{3} & 0\\ -1 & -1 & 2\\ \sqrt{2} & \sqrt{2} & \sqrt{2}\end{pmatrix}, \tag{1}$$

Arrows in Fig. 1(c) represents the local effective magnetic (exchange) field at Mo sites, which is composed of the ferromagnetic exchange field from Mo $3d$ electrons and the exchange field from Nd $4f$ electrons. Under the magnetic field parallel to (1,1,1) direction, below the Néel temperature of Nd sites, the directions of the local exchange fields at sites A, B, and C in the XYZ coordinates are $(\phi_A=\pi/6,\theta)$, $(\phi_B=5\pi/6,\theta)$, and $(\phi_C=3\pi/2,\theta)$, respectively.[17–19] The tilting angle θ changes from $-1.5°$ $(H\to+0$ T) to $+1.5°$ $(H\sim 6$ T) in $Nd_2Mo_2O_7$, corresponding to the change in the spin-ice state at Nd sites.[18,21]

Here, we present a discussion of symmetry. If we rotate the lattice by π around site C in Fig. 1(b), the local exchange field is changed from $\theta=\theta_0>0$ to $-\theta_0$. Since the conductivity tensor is unchanged by the π rotation, the AHC due to spin chirality mechanism is an even function of θ.[14,15] However, O sites in Fig. 1(b) are changed by the π rotation around site C, which means that the Mo $3d$ orbital state is changed. Therefore, the AHC in pyrochlore compounds due to orbital AB phase can have a θ-linear term.

The t_{2g}-orbital kagome lattice model is given by

$$H=\sum_{i\alpha,j\beta,\sigma} t_{i\alpha,j\beta}c^{\dagger}_{i\alpha,\sigma}c_{j\beta,\sigma}-\sum_{i\alpha,\sigma\sigma'}\boldsymbol{h}_i\cdot[\boldsymbol{\mu}_e]_{\sigma,\sigma'}c^{\dagger}_{i\alpha,\sigma}c_{i\alpha,\sigma'}$$
$$+\lambda\sum_{i\alpha\beta,\sigma\sigma'}[\boldsymbol{l}]_{\alpha,\beta}\cdot[\boldsymbol{s}]_{\sigma,\sigma'}c^{\dagger}_{i\alpha,\sigma}c_{i\beta,\sigma'}, \tag{2}$$

where i,j represent the sites, α,β represent the t_{2g} orbitals (xy,yz,zx), and $\sigma,\sigma'=\pm 1$. $t_{i\alpha,j\beta}$ is the hopping integrals between (i,α) and (j,β). The direct d-d hopping integrals are given by the Slater-Koster (SK) parameters $(dd\sigma)$, $(dd\pi)$, and $(dd\delta)$. The third term in Eq. (2) represents the SOI, where λ is the coupling constant, and $\boldsymbol{l}$ and $\boldsymbol{s}$ are the spin and the d-orbital operators. Their matrix elements are given in Ref. 8. For convenience in calculating the AHC, we take the Z axis for the spin quantization axis, where $[s_X,s_Y,s_Z]\times 2$ becomes the Pauli matrix vector. Then, $(s_x,s_y,s_z)=[s_X,s_Y,s_Z]\hat{O}$. The second term in Eq. (2) represents the Zeeman term, where $\boldsymbol{h}_i$ is the local exchange field at site i. $\boldsymbol{\mu}_e\equiv-2\boldsymbol{s}$ is the magnetic moment of an electron.

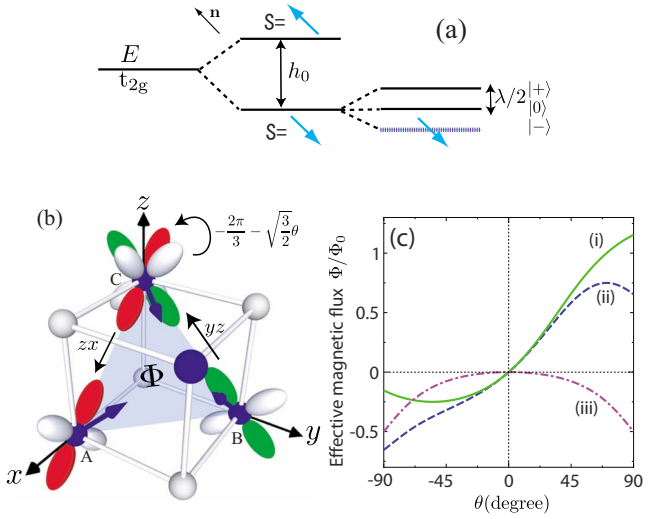

FIG. 2. (Color online) (a) Eigenenergies for t_{2g} electron under the exchange field $\boldsymbol{h}$ and the SOI $(-\lambda/2)\boldsymbol{n}\cdot\boldsymbol{l}$. (b) Orbital AB phase given by the complex t_{2g} orbital wave function at site C. (c) Fictitious magnetic flux due to orbital AB effect (i), due to spin chirality (ii), and the total flux (iii).

The Green's function is given by a 18×18 matrix $\hat{G}_{\boldsymbol{k}}(\epsilon)=[(\epsilon+\mu)\hat{1}-\hat{H}_{\boldsymbol{k}}]^{-1}$, where μ is the chemical potential and $\hat{H}_{\boldsymbol{k}}$ is the matrix for the Hamiltonian in the momentum space. According to the linear-response theory, the AHC is given by $\sigma_{AH}=\sigma^{I}_{AH}+\sigma^{II}_{AH}$ (Ref. 22), where

$$\sigma^{I}_{AH}=\frac{1}{2\pi N}\sum_{\boldsymbol{k}}\mathrm{Tr}[\hat{j}_X\hat{G}^R\hat{j}_Y\hat{G}^A]_{\epsilon=0}, \tag{3}$$

$$\sigma^{II}_{AH}=\frac{-1}{4\pi N}\sum_{\boldsymbol{k}}\int_{-\infty}^{0}d\epsilon$$
$$\times\mathrm{Tr}\left[\hat{j}_X\frac{\partial\hat{G}^R}{\partial\epsilon}\hat{j}_Y\hat{G}^R-\hat{j}_X\hat{G}^R\hat{j}_Y\frac{\partial\hat{G}^R}{\partial\epsilon}-\langle R\to A\rangle\right], \tag{4}$$

where $\hat{G}^{R(A)}_{\boldsymbol{k}}(\epsilon)\equiv\hat{G}_{\boldsymbol{k}}(\epsilon+(-)i\gamma)$ is the retarded (advanced) Green's function. $j_{\boldsymbol{k}\mu}\equiv-e\partial\hat{H}_{\boldsymbol{k}}/\partial k_\mu$ $(\mu=X,Y)$ is the charge current. Since all the matrix elements in $j_{\boldsymbol{k}\mu}$ are odd with respect to $\boldsymbol{k}$, the current vertex correction due to local impurities vanishes identically.[4,8] In the band-diagonal representation, Eqs. (3) and (4) are transformed into Eqs. (30), (32), and (33) in Ref. 4.

Before proceeding to the numerical results, we explain an intuitive reason why prominent AHE is induced by the non-collinearity of the local exchange field $\boldsymbol{h}_i$. For this purpose, we assume the strong-coupling limit where the Zeeman energy is much larger than Fermi energy E_F and the SOI. Since $\boldsymbol{\mu}_e=-2\boldsymbol{s}$, the SOI term at site i is replaced with $(-\lambda/2)\boldsymbol{l}\cdot\boldsymbol{n}_i$, where $\boldsymbol{n}_i\equiv\boldsymbol{h}_i/|\boldsymbol{h}_i|$. Its eigenenergies in the t_{2g} space are 0 and $\pm\lambda/2$, as shown in Fig. 2(a). The eigenstate for $E=-\lambda/2$ is given by

TABLE I. Phases for t_{2g} orbitals in Eq. (5) up to $O(\theta)$.

	ψ_{xy}^{Ξ}	ψ_{yz}^{Ξ}	ψ_{zx}^{Ξ}
$\Xi=A$	$\frac{2\pi}{3}-\frac{1}{2}\sqrt{\frac{3}{2}}\theta$	0	$-\frac{2\pi}{3}+\frac{1}{2}\sqrt{\frac{3}{2}}\theta$
$\Xi=B$	$\frac{2\pi}{3}+\sqrt{\frac{3}{2}}\theta$	0	$-\frac{2\pi}{3}+\frac{1}{2}\sqrt{\frac{3}{2}}\theta$
$\Xi=C$	$\frac{2\pi}{3}-\frac{1}{2}\sqrt{\frac{3}{2}}\theta$	0	$-\frac{2\pi}{3}-\sqrt{\frac{3}{2}}\theta$

$$|\boldsymbol{n}\rangle=\frac{1}{\sqrt{2(n_x^2+n_y^2)}}[-(n_xn_z-in_y)|xy\rangle+(n_y^2+n_z^2)|yz\rangle-(n_xn_y+in_z)|zx\rangle], \quad (5)$$

where $\boldsymbol{n}=(n_x,n_y,n_z)$ in the xyz coordinates: $\boldsymbol{n}_{\Xi}$ ($\Xi=A,B,C$) in the xyz coordinates is given by $[\sin\theta\cos\phi_{\Xi},\sin\theta\cos\phi_{\Xi},\cos\theta]\hat{O}$. When $\theta=0$ ($n_{x,y,z}=1/\sqrt{3}$), Eq. (5) becomes $[\omega|xy\rangle+|yz\rangle+\omega^*|zx\rangle]/\sqrt{3}$, where $\omega=\exp(i2\pi/3)$. Considering that $|\theta|\sim 0.01$ in $Nd_2Mo_2O_7$,[18] we expand Eq. (5) up to the first order in θ. For site C, it is given as $|C\rangle=[(1+\frac{\theta}{\sqrt{2}})\omega e^{-i(1/2)(\sqrt{3/2})\theta}|xy\rangle+(1-\frac{\theta}{2\sqrt{2}})|yz\rangle+(1-\frac{\theta}{2\sqrt{2}})\omega^* e^{-i(\sqrt{3/2})\theta}|zx\rangle]/\sqrt{3}$. Table I shows the phases for $|\alpha\rangle$ orbital at site Ξ in the eigenstate in Eq. (5), ψ_{α}^{Ξ}, up to $O(\theta)$.

Here, we explain that a moving electron acquires the "orbital AB phase," which gives rise to the prominent AHE that is sensitively controlled by the tilting angle θ. Figure 2(b) shows the motion of an electron that enters into site C via yz orbital and exit via zx orbital. When the electron is in the eigenstate $|C\rangle$, the electron acquires the phase difference between yz and zx orbitals, $\exp[i(\psi_{zx}^{C}-\psi_{yz}^{C})]=\omega^* e^{-i(\sqrt{3/2})\theta}$, which is the orbital AB phase that is controlled by θ. The total orbital AB phase factor for the triangle path along $A\rightarrow B\rightarrow C\rightarrow A$ in Fig. 2(b) is given by the phase of the following amplitude:

$$T_{\mathrm{orb}}=\langle A|H_0|C\rangle\langle C|H_0|B\rangle\langle B|H_0|A\rangle, \quad (6)$$

where H_0 is the kinetic term. Here, we take only the most largest SK parameter $(dd\sigma)$ and neglect $(dd\pi)$ and $(dd\delta)$ to simplify the discussion. In this case, only the following intraorbital hoppings exist: $\langle B;xy|H_0|A;xy\rangle=\langle C;yz|H_0|B;yz\rangle=\langle A;zx|H_0|C;zx\rangle=t$. By concentrating only on the phase given in Table I, we obtain

$$T_{\mathrm{orb}}\sim(t^3/27)e^{i(\psi_{zx}^{C}-\psi_{yz}^{C})+i(\psi_{yz}^{B}-\psi_{xy}^{B})+i(\psi_{xy}^{A}-\psi_{zx}^{A})}=(t^3/27)\exp[-i3(\sqrt{3/2})\theta]+O(\theta^2). \quad (7)$$

T_{orb} is also expressed as $T_{\mathrm{orb}}=|T_{\mathrm{orb}}|e^{-i2\pi\Phi_{\mathrm{orb}}/\Phi_0}$, where $\Phi_0=2\pi\hbar/|e|$ is the flux quantum and Φ_{orb} is the "fictitious magnetic flux" due to the orbital AB effect. Therefore, $\Phi_{\mathrm{orb}}=(3/2\pi)(\sqrt{3/2})\theta\,\Phi_0$ up to $O(\theta)$. Since the relation $\Phi_{\mathrm{orb}}\propto\theta$ also holds in pyrochlore compounds, the orbital AB flux should give rise to the AHE that is linear in θ in $Nd_2Mo_2O_7$. Line (i) in Fig. 2(c) represents Φ_{orb} for $|\theta|\leq\pi/2$, which is given by using Eq. (6) and the relationship $-(\Phi_0/2\pi)\mathrm{Im}\ln(T_{\mathrm{orb}}/|T_{\mathrm{orb}}|)$. At $\theta=\pm\pi/2$, the obtained Φ_{orb} is not an integer multiple of $\Phi_0/2$. This fact means that the AHC is finite even in the case of coplanar order.

In the above discussion, we have neglected interorbital hopping integrals for simplicity. If we include them, the AHC is finite even if $\theta=0$ since the orbital AB phase is nonzero, as discussed in Refs. 4 and 7. Thus, interorbital hopping integrals are necessary to realize the AHE for $\theta=0$ (conventional KL-type AHE).

We also discuss the fictitious magnetic flux due to the spin chirality, which comes from the Berry phase accompanied with the spin rotation due to the electron hopping.[14] Line (ii) in Fig. 2(c) represents the fictitious magnetic flux due to the spin chirality Φ_{spin}: geometrically, $-4\pi\Phi_{\mathrm{spin}}$ corresponds to the solid angle subtended by $\boldsymbol{n}_{\mathrm{A}}$, $\boldsymbol{n}_{\mathrm{B}}$, and $\boldsymbol{n}_{\mathrm{C}}$. Since $\Phi_{\mathrm{spin}}\propto\theta^2$ for $\theta\ll 1$, spin chirality mechanism is negligible in $Nd_2Mo_2O_7$.[18] Line (iii) shows the total flux $\Phi_{\mathrm{tot}}=\Phi_{\mathrm{orb}}+\Phi_{\mathrm{spin}}$.

Thus, all the upward and the downward ABC triangles in Fig. 1(b) are penetrated by Φ_{tot}. However, the total flux in the unit cell cancels out since the hexagons are penetrated by $-2\Phi_{\mathrm{tot}}$. Nonetheless, the AHC becomes finite[14,23] since the contribution from the triangle path, which is the third order of the hopping integrals, would be the most important. The main features of the AHE due to orbital AB effect, $\sigma_{\mathrm{AH}}^{\mathrm{orb}}$, are the following: (a) $\sigma_{\mathrm{AH}}^{\mathrm{orb}}$ dominates the spin chirality AHE for $\theta\ll 1$ and (b) $\sigma_{\mathrm{AH}}^{\mathrm{orb}}$ exists even if $\theta=\pi/2$ (coplanar order), whereas spin chirality AHE vanishes since $\Phi_{\mathrm{spin}}(\theta=\pi/2)=\Phi_0/2$.

From now on, we perform numerical calculation for the AHC using Eqs. (3) and (4), which contain the effects from both Φ_{orb} and Φ_{spin}, and verify that the concept of orbital AB effect is still appropriate even in the weak-coupling regime where $|\boldsymbol{h}_i|\ll E_{\mathrm{F}}$. Here, we put the SK parameters between the nearest-neighbor Mo sites as $(dd\sigma)=-1.0$, $(dd\pi)=0.6$, and $(dd\delta)=-0.1$. $|(dd\sigma)|$ corresponds to 2000 K. The spin-orbit coupling constant for Mo $4d$ electron is $\lambda=0.5$.[8] The number of electrons per site is $n=2$ (1/3 filling) for $Nd_2Mo_2O_7$ since the valence of Mo ion is 4+. To reproduce the magnetization of Mo ion $1.3\mu_{\mathrm{B}}$ in $Nd_2Mo_2O_7$, we set $|\boldsymbol{h}_i|=0.9$. We also put the damping rate $\gamma=0.2-0.5$ to reproduce the resistivity ~ 1 mΩ cm in a single crystal.[19]

Figure 3(a) shows the μ dependence of the AHC for $\theta=-1.5°$ (~ 0 T), $\theta=0$ (~ 3 T), and $\theta=1.5°$ (~ 6 T). The AHC for $\theta=0$ is given by the conventional KL mechanism. Since the present spin structure-driven AHE is linear in θ, a very small θ causes a prominent change in the AHC for $1.3>\mu>-1.3$ $(4.7>n>1.0)$. Since $e^2/ha=10^3$ Ω^{-1} cm^{-1} for $a=4$ Å (a is the interlayer spacing), the AHC for $n=2$ and $\theta=1.5°$ corresponds to 30 Ω^{-1} cm^{-1}, which is consistent with experiments.

Here, we analyze the θ dependence of the AHC in detail, by ignoring the experimental constraint $|\theta|\leq 1.5°$. Figure 3(b) shows the AHCs as functions of θ. Lines (i) and (ii) represent the total AHC in the present model for $\gamma=0.5$ and 0.2, respectively. Their overall functional forms are approximately odd with respect to θ, and it takes a large value even if $\theta=\pm\pi/2$ (coplanar order). These results are consistent with the AHE induced by the orbital AB effect discussed in Fig. 2. Note that $\gamma>0.2$ corresponds to "high-resistivity regime" where the intrinsic AHC follows an approximate scaling relation $\sigma_{\mathrm{AH}}\propto\rho^2$.[2,4] Line (iii) in Fig. 3(b) shows the AHC in the s-orbital model studied in Ref. 15. We put the nearest-neighbor hopping $t=-0.8$, $\gamma=0.5$, and $|\boldsymbol{h}|=0.9$. We also put

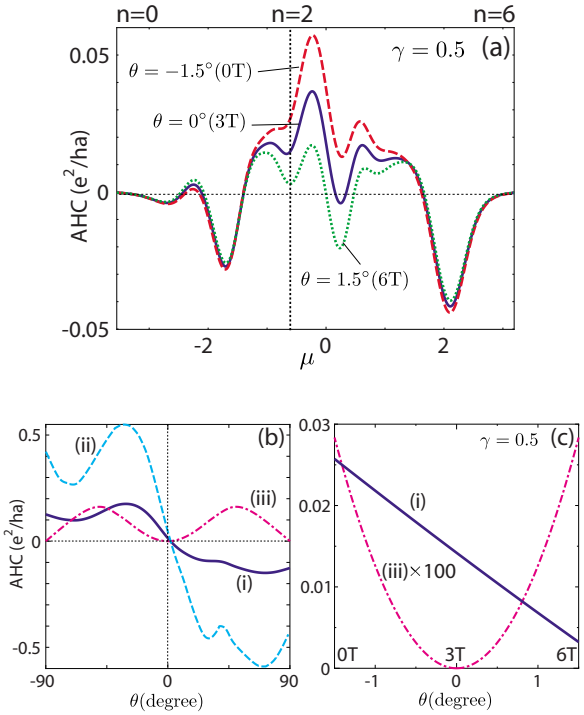

FIG. 3. (Color online) (a) AHC for $\theta=0$ and $\pm 1.5°$ as function of μ. (b) AHC in the present t_{2g}-orbital model for (i) $\gamma=0.5$ and (ii) $\gamma=0.2$. (iii) shows the AHC in the s-orbital model for $\gamma=0.5$. (c) (i) and (iii) for $|\theta| \leq 1.5°$.

$n=2.5/3=0.83$ since $n=2/3$ (1/3 filling) corresponds to band insulating state.[15] Although the obtained AHC takes a large value for $\theta \sim 50°$, it is 100 times smaller than the AHC in the t_{2g} model (i) for $|\theta| \leq 1.5°$, as shown in Fig. 3(c).

Here, we make comparison with the theory and experiments for $Nd_2Mo_2O_7$: under $\boldsymbol{H} \| (1,1,1)$ below T_N, σ_{AH} decreases with H monotonically from $H \to 0$ T ($\theta \approx -1.5°$) to 6 T ($\theta \approx 1.5°$). This experimental result is consistent with the AHE due to the orbital AB effect that is linear in θ. The present study also reproduces the experimental phenomenological equation $\rho_H^{AHE}=4\pi R_s M_Z^{Mo}+4\pi R_s' M_Z^{Nd}$: the first term is the conventional KL term ($\theta=0$) and the second term is the θ-linear term since $\theta \propto \sqrt{h_X^2+h_Y^2}$ and $\sqrt{h_X^2+h_Y^2} \propto M_Z^{Nd}$ due to noncoplanar magnetic order of Nd moment.[18,21]

The realization condition for the spin structure driven AHE in the present t_{2g} model is much more general than that in the s-orbital model. For example, the AHC is finite even in the coplanar spin state ($M_z=0$), in high contrast to the chirality-driven AHE. Moreover, according to Eq. (7), orbital AB phase emerges if only one of $\theta_A, \theta_B, \theta_C$ is nonzero. Therefore, in the present t_{2g} model, prominent AHE due to noncollinearity is realized unless $\boldsymbol{n}_A \| \boldsymbol{n}_B \| \boldsymbol{n}_C$, with the aid of the orbital AB effect and the SOI.

In summary, we studied the AHE in the t_{2g}-orbital model in the presence of noncollinear magnetic configurations. Thanks to the SOI, local exchange field modifies the complex d-orbital wave function, and the resultant Berry phase induces prominent AHE that is much larger than the chirality-driven AHE. Since the derived AHC is linear in the tilting angle of Mo moment, θ, experimental large field dependence in $Nd_2Mo_2O_7$ is reproduced.

We are grateful to M. Sato and Y. Yasui for valuable discussions. This work was supported by Grant-in-Aid for Scientific Research on Priority Areas "Novel States of Matter Induced by Frustration." We also acknowledge hospitality of STCM-Kyoto in Yukawa Institute in 2008.

[1] R. Karplus and J. M. Luttinger, Phys. Rev. **95**, 1154 (1954); J. M. Luttinger, *ibid.* **112**, 739 (1958).
[2] H. Kontani and K. Yamada, J. Phys. Soc. Jpn. **63**, 2627 (1994).
[3] Y. Yao, L. Kleinman, A. H. MacDonald, J. Sinova, T. Jungwirth, D. S. Wang, E. Wang, and Q. Niu, Phys. Rev. Lett. **92**, 037204 (2004).
[4] Hiroshi Kontani, Takuro Tanaka, and Kosaku Yamada, Phys. Rev. B **75**, 184416 (2007).
[5] A. A. Kovalev, K. Vyborny, and J. Sinova, Phys. Rev. B **78**, 041305(R) (2008).
[6] J. I. Inoue, T. Kato, Y. Ishikawa, H. Itoh, G. E. W. Bauer, and L. W. Molenkamp, Phys. Rev. Lett. **97**, 046604 (2006).
[7] H. Kontani, T. Tanaka, D. S. Hirashima, K. Yamada, and J. Inoue, Phys. Rev. Lett. **100**, 096601 (2008).
[8] T. Tanaka, H. Kontani, M. Naito, T. Naito, D. S. Hirashima, K. Yamada, and J. Inoue, Phys. Rev. B **77**, 165117 (2008).
[9] H. Kontani, T. Tanaka, D. S. Hirashima, K. Yamada, and J. Inoue, Phys. Rev. Lett. **102**, 016601 (2009).
[10] C. Wu, Phys. Rev. Lett. **101**, 186807 (2008).
[11] G. Sundaram and Q. Niu, Phys. Rev. B **59**, 14915 (1999).
[12] M. Onoda and N. Nogaosa, J. Phys. Soc. Jpn. **71**, 19 (2002).
[13] Jinwu Ye, Yong Baek Kim, A. J. Millis, B. I. Shraiman, P. Majumdar, and Z. Tesanovic, Phys. Rev. Lett. **83**, 3737 (1999).
[14] K. Ohgushi, S. Murakami, and N. Nagaosa, Phys. Rev. B **62**, R6065 (2000).
[15] M. Taillefumier, B. Canals, C. Lacroix, V. K. Dugaev, and P. Bruno, Phys. Rev. B **74**, 085105 (2006).
[16] G. Tatara and H. Kawamura, J. Phys. Soc. Jpn. **71**, 2613 (2002).
[17] S. Yoshii, S. Iikubo, T. Kageyama, K. Oda, Y. Kondo, K. Murata, and M. Sato, J. Phys. Soc. Jpn. **69**, 3777 (2000).
[18] Y. Yasui, T. Kageyama, T. Moyoshi, M. Soda, M. Sato, and K. Kakurai, J. Phys. Soc. Jpn. **75**, 084711 (2006).
[19] Y. Taguchi, Y. Oohara, H. Yoshizawa, N. Nagaosa, and Y. Tokura, Science **291**, 2573 (2001); Y. Taguchi, T. Sasaki, S. Awaji, Y. Iwasa, T. Tayama, T. Sakakibara, S. Iguchi, T. Ito, and Y. Tokura, Phys. Rev. Lett. **90**, 257202 (2003).
[20] Y. Machida, S. Nakatsuji, Y. Maeno, T. Tayama, T. Sakakibara, and S. Onoda, Phys. Rev. Lett. **98**, 057203 (2007).
[21] M. Sato and Y. Yasui (private communication).
[22] P. Streda, J. Phys. C **15**, L717 (1982); N. A. Sinitsyn, A. H. MacDonald, T. Jungwirth, V. K. Dugaev, and J. Sinova, Phys. Rev. B **75**, 045315 (2007).
[23] F. D. M. Haldane, Phys. Rev. Lett. **61**, 2015 (1988).